



ChemComm

Supramolecular ultrafast energy and electron transfer in a directly linked BODIPY-oxoporphyrinogen dyad upon fluoride ion binding

Journal:	<i>ChemComm</i>
Manuscript ID	CC-COM-01-2020-000633.R2
Article Type:	Communication

SCHOLARONE™
Manuscripts

Supramolecular ultrafast energy and electron transfer in a directly linked BODIPY-oxoporphyrinogen dyad upon fluoride ion binding[†]

Mandeep K. Chahal,^{*a} Anuradha Liyanage,^b Habtom B. Gobeze,^b Daniel T. Payne,^a Katsuhiko Ariga,^a Jonathan P. Hill,^{*a} and Francis D'Souza^{*b}

⁵ Received (in XXX, XXX) Xth XXXXXXXXXX 200X, Accepted Xth XXXXXXXXXX 200X

First published on the web Xth XXXXXXXXXX 200X

DOI: 10.1039/b000000x

A directly linked BODIPY-oxoporphyrinogen dyad has been newly synthesized and occurrence of sequential photoinduced energy and electron transfer upon fluoride anion binding to oxoporphyrinogen has been demonstrated by spectral, electrochemical and femtosecond transient absorption studies.

The outstanding structure-function-reactivity relationship that exists for naturally occurring photosynthetic reaction centres¹ has motivated the design and synthesis of a large number of covalently-linked and self-assembled conjugates including dyads, triads, tetrads and pentads.² These synthetic model systems have been used to mimic energy- and electron-transfer events often leading to charge-separated states where sufficient energy is stored for photocatalytic processes targeted for light-to-fuel conversion.²⁻³ The presence of additional factors such as protons, metal cations and anions at appropriate binding sites of the donor-acceptor complexes is known to modulate redox properties of the latter thereby promoting excited state electron transfer events and prolonging the lifetime of the electron transfer products, i.e., the radical ion-pairs.⁴ In this regard, the effects of external ionic cofactors on the efficacy of electron transfer processes is a well-known phenomenon in biological systems. For example, calcium cations and chloride anions are known to be essential cofactors for efficient water oxidation in the oxygen evolving complex of photosystem-II.⁵

Oxoporphyrinogen (OxP), a macrocycle belonging to the xanthoporphyrinogen family, is known for its broad intense absorption in the visible region due to its extended conjugation.⁶ OxP and its N-alkylated derivatives are relatively difficult to oxidize beyond their native states but can still exist in a variety of redox states.⁷ Central pyrrolic NH groups of OxP can also interact with a variety of anions leading to modulation of its spectral and electrochemical properties.⁸ By taking advantage of these properties, we have previously been able to observe intrasupramolecular complex excited state electron transfer in oligochromophoric model systems containing sites for photosensitizer, zinc porphyrin(s), and anion binding at the macrocycle core in the presence of an appropriately substituted fullerene coordinated to zinc porphyrin as an electron acceptor.⁹ Anion binding has also been found to improve photoelectrochemical responses in a zinc porphyrin-oxoporphyrinogen modified TiO₂ solar cell,¹⁰ and in relevant donor-acceptor conjugates.¹¹ Thus, chemically functionalized OxPs have provided a unique

opportunity to build novel supramolecular systems to probe photo-induced events in the presence of external factors, which are otherwise difficult or impossible to observe.

In this work, we have further explored the novelty of OxP for modulation of energy and electron transfer events upon anion binding in a directly linked donor-acceptor dyad. The well-known photosensitizer, 4,4-difluoro-4-bora-3a,4a-diazas-indacene (BODIPY)¹² is linked directly at the β-pyrrole position of N₂₁,N₂₃-biphenyl-appended OxP (Fig. 1). Direct linkage improves any potential interchromophore electronic communication, while blocking two pyrrole N atoms not only fixes the macrocyclic conformation but also leaves two calix[4]pyrrole type NH groups available for binding an anionic cofactor, here fluoride anion.⁸⁻¹¹ Photo-excitation of BODIPY-OxP leads to charge separation involving oxidation of the anion-interacting OxP unit to its cation radical, which is promoted by the presence of the charge-balancing fluoride anion, in turn stabilizing BODIPY⁻-OxP⁺·F⁻ radical ion pair, demonstrated here using spectroscopic, electrochemical and transient absorption studies.

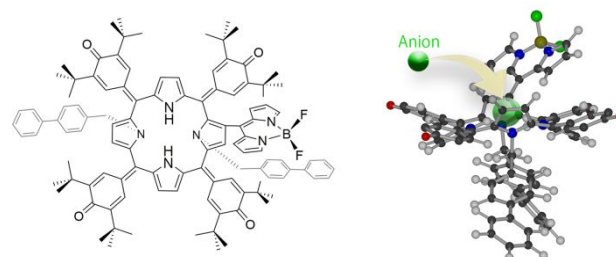


Fig. 1. Chemical structure (left) of the BODIPY-OxP dyad synthesized to visualize anion-binding-promoted excited state electron transfer in the present study. Model (right) of the anion binding site (t-butyl groups omitted for clarity).

Details of the synthesis of BODIPY-OxP dyad are given in the Supplementary Information. Briefly, *rac*-2-formyl-N₂₁,N₂₃-(4-bromobenzyl)-OxP¹³ was reacted with 80 phenylboronic acid under Suzuki coupling conditions¹⁴ (to eliminate the bromine atoms) followed by condensation of the formyl group with pyrrole and reaction with BF₃·Et₂O under standard conditions for formation of the BODIPY unit.¹⁵ A racemic mixture of the product was then used for all analyses.

The absorption spectrum of the dyad along with the control compounds (in *o*-dichlorobenzene, DCB) is shown in Fig. 2a. Both OxP and BODIPY absorb in the same wavelength

region, although the absorption due to BODIPY is substantially sharper than that of OxP. The peak maxima of the BODIPY control is centred at 505 nm while that for the OxP control is at 510 nm. The dyad exhibits absorption maximum at 494 nm with broad shoulders either side of this. The dyad has absorption over the 300 – 650 nm range making it a wide-band capturing dyad. Fluorescence emission of BODIPY and OxP controls occurs with maxima respectively at 526 nm and 718 nm (Fig. 2b) while the BODIPY-OxP dyad emission spectrum contains two peaks at 506 and 714 nm due to the presence of the two fluorophores. BODIPY emission is significantly quenched (82 %) in the dyad over the BODIPY control already indicating occurrence of excited state events such as energy or electron transfer from $^1\text{BODIPY}^*$ to OxP.¹⁶

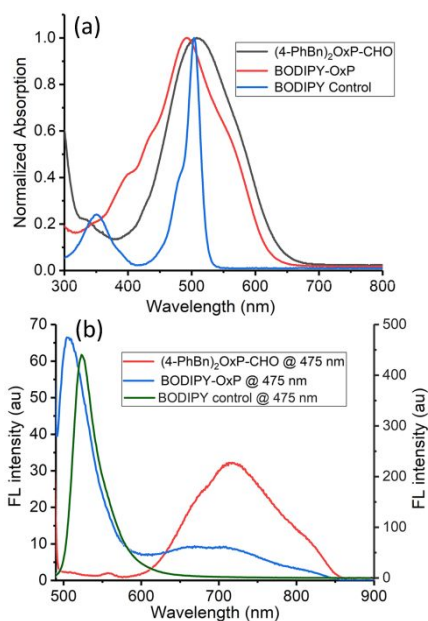


Fig. 2. (a) Normalized electronic absorption and (b) fluorescence emission spectra of the BODIPY-OxP dyad and controls in DCB ($c = 0.5 \times 10^{-5}$ M, $\lambda_{\text{exc}} = 475$ nm). Emission intensity of the BODIPY control is indicated on the Y-axis at right in (b).

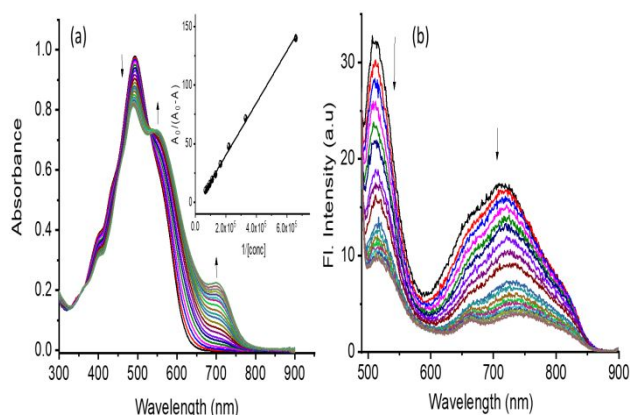


Fig. 3. Variation in (a) electronic absorption and (b) fluorescence ($\lambda_{\text{exc}} = 465$ nm) spectra of BODIPY-OxP dyad during addition of F^- (1 μL aliquots of 0.01 M tetrabutylammonium (TBA) fluoride solution) to form the BODIPY-OxP:F⁻ complex. Inset of (a): Benesi-Hildebrand plot constructed to evaluate the binding constant.

Fluoride anion binding (see also Fig. S1) and its effects on fluorescence emission of the dyad were then investigated. Spectral variations associated with F^- binding at OxP is shown in Fig. 3a. These are typical for anion binding to OxP and involve new peaks at 552 and 700 nm accompanied by isosbestic points at 332 and 360 nm were observed. The Benesi-Hildebrand method applied to these data¹⁷ yield a binding constant of 2.0×10^4 M⁻¹ was obtained for a 1:1 complex (see Fig. 3a inset for the plot). As shown in Fig. 3b, F^- binding causes further quenching of both BODIPY and OxP emission, again indicating the occurrence of excited state events in the BODIPY-OxP:F⁻ supramolecular complex.¹⁶

To determine the quenching mechanism in the dyad in the absence/presence of F^- , electrochemical studies were performed to evaluate the redox potentials of the compounds in DCB containing 0.1 M (TBA)ClO₄. Fig. 4a shows that the first oxidation and first reduction of BODIPY control are at 1.26 and -1.15 V, respectively, while for the OxP control the corresponding processes are at 0.659 and -1.47 V (all vs. internal standard Fc/Fc⁺). The easy reduction of BODIPY and corresponding easy oxidation of OxP establish their respective roles as electron acceptor and electron donor. In the dyad, the first oxidation at 0.60 V (due to OxP) and first reduction at -1.27 V (due to BODIPY) were then observed. Subsequent addition of F^- facilitates oxidation of OxP¹⁸ in the BODIPY-OxP:F⁻ supramolecular complex. In the complex, OxP oxidation at 0.23 V and BODIPY reduction at -1.29 V vs. Fc/Fc⁺ were observed.

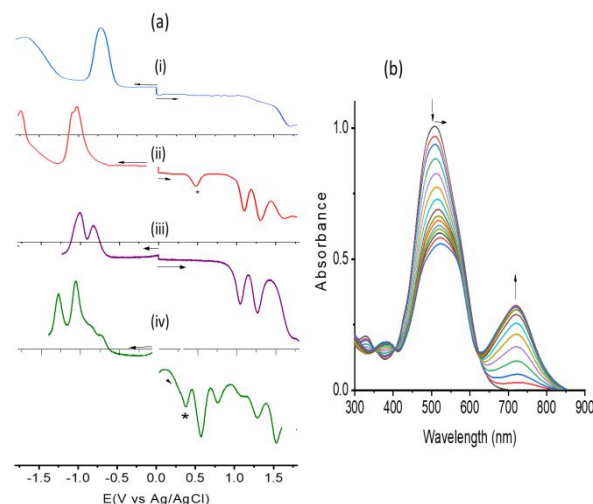
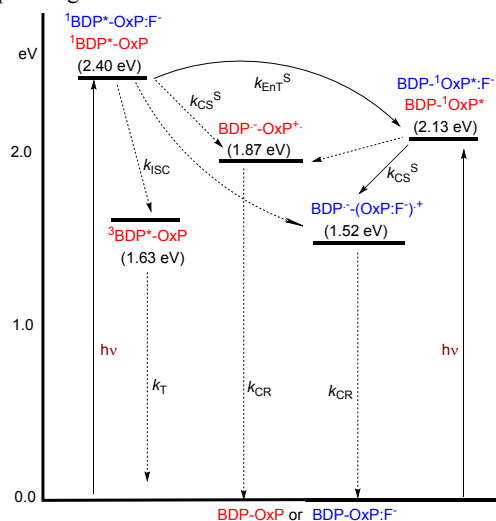


Fig. 4. (a) Differential pulse voltammograms of (i) BODIPY control, (ii) OxP control, (iii) BODIPY-OxP dyad, and (iv) BODIPY-OxP:F⁻ supramolecular complex in DCB containing 0.1 M (TBA)ClO₄. * indicates internal standard ferrocene. Scan rate = 5 mV/s, pulse width = 0.25 s, pulse height = 0.025 V. (b) Spectral changes observed during chemical oxidation of OxP control in DCB (nitrosonium hexafluorophosphate was used as an oxidizing agent).

Free-energies of excited state charge transfer from $^1\text{BODIPY}^*$ and $^1\text{OxP}^*$ were estimated from these spectral and electrochemical data using the Rehm-Weller approach,¹⁹ and an energy level diagram was constructed to visualize different photoinduced energy or electron transfer events, as shown in Fig. 5. From the energy level diagram, it is clear that excited

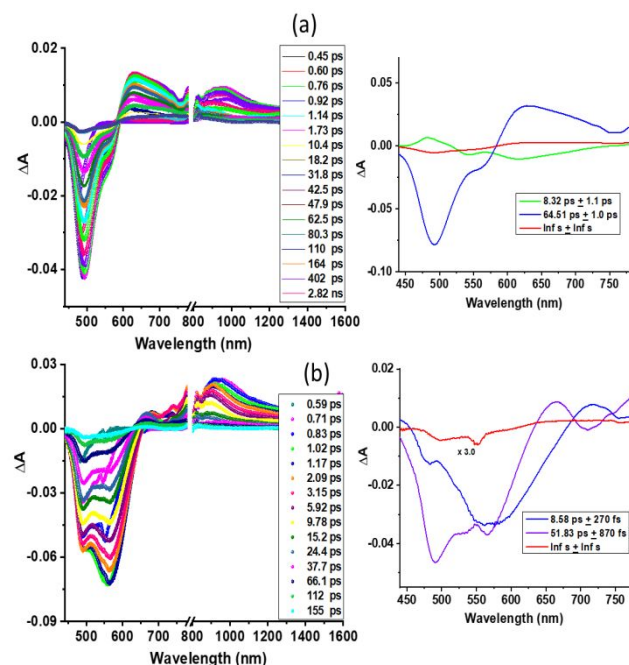
state energy transfer from $^1\text{BODIPY}^*$ to OxP is thermodynamically possible. Electron transfer is also possible from both $^1\text{BODIPY}^*$ and $^1\text{OxP}^*$ states in the BODIPY-OxP dyad and the BODIPY-OxP:F⁻ supramolecular complex yielding respectively BODIPY⁻-OxP⁺ and BODIPY⁻-OxP⁺:F⁻ charge separated species. The charge separated state, BODIPY⁻-OxP⁺, is higher in energy than the triplet state of both BODIPY (1.63 eV).²⁰ Under this condition, the charge separated state might relax to the ground state through the $^3\text{BODIPY}^*$ state. Interestingly, the energy of the BODIPY⁻-OxP⁺:F⁻ state is lower than that of $^3\text{BODIPY}^*$, and it can relax directly to the ground state. Since OxP⁺ is predicted to be the electron transfer product, in order to characterize this species, the OxP control compound was chemically oxidized as shown in Fig. 4b with a new peak emerging at 722 nm being assigned as due to OxP⁺. Spectroelectrochemical reduction of BODIPY yields peaks at 460 and 560 nm corresponding to BODIPY⁻.²¹



20 Fig. 5. Energy level diagram depicting different photoinduced electron transfer events in the dyad. Abbreviations: CS = charge separation, CR = charge recombination, S = singlet state and T = triplet state. Solid arrow = major path, dashed arrow = minor path.

Femtosecond transient absorption spectroscopy (fs-TA) was performed on the compounds as molecular excited states evolve on this timescale. First, fs-TA measurements on the two control compounds was performed, as shown in Fig. S2 in ESI. For the BODIPY control, instantaneously formed $^1\text{BODIPY}^*$ has a negative peak at 509 nm due to contributions from ground state bleaching (GSB) and stimulated emission (SE) (Fig. S2a). In the near-IR region, a broad positive signal was observed at 1160 nm attributed to excited state absorption (ESA). Decay/decay of positive/negative signals was accompanied by a broad signal in the 500-700 nm range that is attributed to $^3\text{BODIPY}^*$ formed by intersystem crossing (ISC). Decay associated spectra (DAS) generated from global analysis reveal two components: that at 13 ps is attributed to relaxation and solvation of the initially formed $^1\text{BODIPY}^*$ with the second at 524 ps representing decay of relaxed $^1\text{BODIPY}^*$. For OxP control, the spectra contain a negative peak at 506 nm due to GSB and SE and positive peaks at 663

and 992 nm attributed to ESA of $^1\text{OxP}^*$ (Fig. S2b). DAS revealed four components with the first at 246 fs (close to the detection limit of our instrumental setup), possibly due to higher excited states, being neglected. DAS at 8 ps is attributed to relaxation and solvation of initially formed $^1\text{OxP}^*$ while the 91 ps DAS is due to $^1\text{OxP}^*$. The long-lived DAS (> 3 ns) is attributed here to $^3\text{OxP}^*$ formed by ISC.



50 Fig. 6. Fs-TA spectra at the indicated delay times of (a) OxP-BODIPY ($\lambda_{\text{exc}} = 482$ nm) and (b) BODIPY-OxP:F⁻ ($\lambda_{\text{exc}} = 482$ nm) in deaerated DCB. DAS from global analysis is shown at right.

Fs-TA spectra of the BODIPY-OxP dyad are shown in Fig. 6a. TA spectra contain features of both species due to the strong coincidence of the absorption of OxP and BODIPY moieties (Fig. 2a). Despite this, close examination of the transient data revealed initial formation of $^1\text{BODIPY}^*$ within the initial 1 ps. Fast recovery of GSB of $^1\text{BODIPY}^*$ results in emergence of GSB of OxP in less than 2 ps suggesting singlet-singlet energy transfer from $^1\text{BODIPY}^*$ to OxP in the dyad. This energy transfer process is thermodynamically feasible, as shown in Fig. 5, and the small time constant for this event is reasonable given the direct linking of the π -systems of the two donor-acceptor entities.²² DAS yields four spectra, the first of which at 200 fs is within the temporal resolution of our instrumental setup and is not shown. Interestingly, spectral shapes and time constants (8 and 66 ps) of the next two DAS spectra are close to that of the OxP control. DAS on an infinite time scale also resemble that of the OxP control. This suggests that the $^1\text{OxP}^*$ formed in the dyad is not involved in electron transfer to produce the BODIPY⁻-OxP⁺ charge separated state.

Fs-TA spectra of BODIPY-OxP:F⁻ supramolecular complex is shown in Fig. 6b. Transient spectral features depart significantly from the BODIPY-OxP dyad alone with there being evidence for energy transfer within the initial 1.2 ps. In

the complex, GSB of Oxp:F⁻ is red-shifted to 566 nm while the ESA is blue-shifted initially to 931 nm then to 894 nm due to vibrational cooling. Importantly, recovery/decay of GSB/ESA reveals new peaks characteristic of BODIPY⁻ in the 550 nm range and new peaks corresponding to Oxp⁺ in the 700-730 nm range. These results indicate occurrence of charge separation leading to a BODIPY⁻-Oxp⁺:F⁻ charge separated state. DAS for this system contains three components: the first of these with 8.6 ps time constant is due to ¹Oxp^{*}:F⁻ while the 52 ps component, which contains signature peaks of both BODIPY⁻ and Oxp⁺ is attributed to the charge separated state. The final >3 ns component has weak spectral features of the long-lived components of pristine BODIPY and Oxp (see Fig. S1), perhaps due to ³BODIPY* or ³Oxp* formed through ISC of a proportion of ¹BODIPY* or ¹Oxp*.

Conclusions

In summary, BODIPY-Oxp dyad with chromophores directly linked at the β-pyrrole positions of Oxp, has been synthesized to mimic the primary events of photosynthesis. Fs-TA studies reveal ultrafast energy transfer in less than 2 ps from ¹BODIPY* to Oxp in the dyad due to the close proximity of the donor and acceptor entities. Binding of fluoride anions F⁻ yields the BODIPY-Oxp:F⁻ supramolecular complex and facilitates oxidation of the Oxp moiety. F⁻-binding induced redox modulation promotes excited state electron transfer in the BODIPY-Oxp:F⁻ complex with the final lifetime of the charge separated state from global analysis of the transient data being about 50 ps. This work further establishes the supramolecular redox modulation approach as being valid for the control of intramolecular energy and electron transfer processes relevant to the mimicking of naturally occurring photochemical events. It also further emphasizes molecular design principles for the introduction of different intramolecular processes. Here, we have exploited the anion interacting site available in N-alkyl Oxp molecules. We have also recently introduced cation binding units to the Oxp core and will report shortly on the effects of cations and even ion pair interactions on the photochemistry of similar systems.

This work was financially supported by the National Science Foundation (Grant No. 1401188 to FD). This work was also partly supported by World Premier International Research Center Initiative (WPI Initiative), MEXT, Japan, JSPS KAKENHI Grant No. JP16H06518 (Coordination asymmetry), and CREST JST, Japan (Grant No. JPMJCR1665).

Conflicts of interest

The authors declare no conflicts of interest.

Notes and references

^aInternational Center for Materials Nanoarchitectonics (WPI-MANA), National Institute of Materials Science (NIMS), Namiki 1-1, Tsukuba, Ibaraki, 305-0044, Japan. E-mail: Chahal.Mandeep@nims.go.jp; Jonathan.Hill@nims.go.jp

^bDepartment of Chemistry, University of North Texas, 1155 Union Circle, #305070, Denton, TX 76203-5017, United States; E-mail: Francis.dsouza@unt.edu

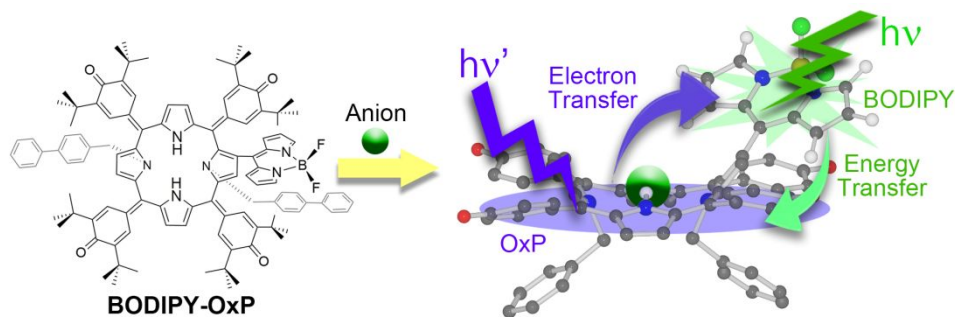
†Electronic Supplementary Information (ESI) available: [synthesis and experimental details, additional fs-TA spectral data]. See DOI: 10.1039/c000000x/

- (a) *The Photosynthetic Reaction Center*; J. Deisenhofer, J. R. Norris, Eds.; Academic Press, New York, 1993; (b) W. Leibl, P. Mathis, *Electron Transfer in Photosynthesis*. Series on Photoconversion of Solar Energy, 2004, **2**, 117.
- (a) D. Gust, T. A. Moore and A. L. Moore, *Acc. Chem. Res.*, 2009, **42**, 1890; (b) M. R. Wasielewski, *Acc. Chem. Res.*, 2009, **42**, 1910; (c) G. Bottari, G. de la Torre, D. M. Guldi and T. Torres, *Chem. Rev.*, 2010, **110**, 6768; (d) D. Kim, *Multiporphyrin Arrays: Fundamentals and Applications*, Pan Stanford Publishing, Singapore, 2012; (e) H. Imahori, T. Umeyama and S. Ito, *Acc. Chem. Res.*, 2009, **42**, 1809; (f) F. D'Souza and O. Ito, *Chem. Soc. Rev.*, 2012, **41**, 86; (g) S. Fukuzumi, *Phys. Chem. Chem. Phys.*, 2008, **10**, 2283; (h) V. Balzani, A. Credi and M. Venturi, *ChemSusChem*, 2008, **1**, 26.
- S. Lewis and D. G. Nocera, *Proc. Natl. Acad. Sci. U. S. A.*, 2006, **103**, 15729.
- (a) S. Fukuzumi, K. Ohkubo, F. D'Souza and J. L. Sessler, *Chem. Commun.*, 2012, **48**, 9801; (b) S. Fukuzumi and K. Ohkubo, *Coord. Chem. Rev.*, 2010, **254**, 373.
- (a) C. F. Yocum, *Coord. Chem. Rev.*, 2007, **252**, 296; (b) J. P. McEvoy and G. W. Brudvig, *Chem. Rev.*, 2006, **106**, 4455; (c) L. M. Utsching and M. C. Thurnauer, *Acc. Chem. Res.*, 2004, **37**, 439.
- L. R. Milgrom, *Tetrahedron*, 1983, **39**, 3895.
- J. P. Hill, I. J. Hewitt, C. E. Anson, A. K. Powell, A. L. McCarty, P. A. Karr, M. E. Zandler and F. D'Souza, *J. Org. Chem.*, 2004, **69**, 5861.
- J. P. Hill, A. L. Schumacher, F. D'Souza, J. Labuta, C. Redshaw, M. R. J. Elsegood, M. Aoyagi, T. Nakanishi and K. Ariga, *Inorg. Chem.*, 2006, **45**, 8288.
- F. D'Souza, N. K. Subbaiyan, Y. Xie, J. P. Hill, K. Ariga, K. Ohkubo and S. Fukuzumi, *J. Am. Chem. Soc.*, 2009, **131**, 16138.
- N. K. Subbaiyan, J. P. Hill, K. Ariga, S. Fukuzumi and F. D'Souza, *Chem. Commun.*, 2011, **47**, 6003.
- W. A. Webre, H. B. Gobeze, S. Shao, P. A. Karr, K. Ariga, J. P. Hill and F. D'Souza, *Chem. Commun.*, 2018, **54**, 1351.
- (a) G. Ulrich, R. Ziessel and A. Harriman, *Angew. Chem. Int. Ed.*, 2008, **47**, 1184; (b) M. El-Khouly, S. Fukuzumi and F. D'Souza, *ChemPhysChem*, 2014, **15**, 30.
- M. K. Chahal, J. Labuta, V. Brezina, P. A. Karr, Y. Matsushita, W. A. Webre, D. T. Payne, K. Ariga, F. D'Souza and J. P. Hill, *Dalton Trans.*, 2019, **48**, 15583.
- N. Miyaura and A. Suzuki, *Chem. Rev.*, 1995, **95**, 2457.
- (a) Y. Chen, L. Wan, D. Zhang, Y. Bian and J. Jiang, *Photochem. Photobiol. Sci.*, 2011, **10**, 1030; (b) S. Swavey, J. Quinn, M. Coladipietro, K. G. Cox and M. K. Brennaman, *RSC Adv.*, 2017, **7**, 173.
- Principles of Fluorescence Spectroscopy*, 3rd ed., Ed.: J. R. Lakowicz, Springer, Singapore, 2006.
- H. A. Benesi and J. H. Hildebrand, *J. Am. Chem. Soc.*, 1949, **71**, 2703.
- A. L. Schumacher, J. P. Hill, K. Ariga and F. D'Souza, *Electrochem. Commun.*, 2007, **9**, 2751.
- D. Rehm and A. Weller, *Isr. J. Chem.* 1970, **8**, 259.
- S. Shao, H. B. Gobeze, V. Bandi, C. Funk, B. Heine, M. J. Duffy, V. Nesterov, P. A. Karr and F. D'Souza, *ChemPhotoChem* 2020, **4**, 68.
- S. J. Hendel, A. M. Poe, P. Khomein, Y. Bae, S. Thayumanavan and E. R. Young, *J. Phys. Chem. A.*, 2016, **120**, 8794.
- (a) J. Follna-Berna, S. Seetharaman, L. Martin-Gomix, G. Charalambidis, A. Trapali, P. A. Karr, A. G. Coutsolelos, F. Fernandez-Lazaro, F. D'Souza and A. Sastre-Santos, *Phys. Chem. Chem. Phys.*, 2018, **20**, 7798; (b) R. Sharma, H. B. Gobeze, F. D'Souza and M. Ravikanth, *ChemPhysChem*, 2016, **17**, 2516.

Table of Contents

Supramolecular ultrafast energy and electron transfer in a directly linked BODIPY-oxoporphyrinogen dyad upon fluoride ion binding †

Mandeep K. Chahal,^{*a} Anuradha Liyanage,^b Habtom B. Gobeze,^b Daniel T. Payne,^a Katsuhiko Ariga,^a Jonathan P. Hill,^{*a} and Francis D'Souza^{*b}



10

Photosynthetic mimicry of sequential ultrafast energy transfer followed by electron transfer upon fluoride binding to the oxoporphyrinogen cavity in a BODIPY-oxoporphyrinogen dyad is demonstrated.

15

20

25